COLD SPRING HARBOR
Molecular Case Studies

RESEARCH REPORT

m.3685T > C is a novel mitochondrial DNA variant that causes Leigh syndrome

Jeffrey Jean,[1] Eirini Christodoulou,[2] Xiaowu Gai,[1,2] Benita Tamrazi,[1,2] Moin Vera,[3] Wendy G. Mitchell,[1,2] and Ryan J. Schmidt[1,2]

[1]Keck School of Medicine of the University of Southern California, Los Angeles, California 90033, USA; [2]Children's Hospital Los Angeles, Los Angeles, California 90027, USA; [3]Kaiser Permanente, Oakland, California 94611, USA

Abstract Variants in the mitochondrial genome can result in dysfunction of Complex I within the electron transport chain, thus causing disruptions in oxidative phosphorylation. Pathogenic variants in the *MT-ND1* (NADH:ubiquinone oxidoreductase core subunit 1) gene that result in Complex I dysfunction are a known cause of Leigh syndrome. The patient is a 4-yr-old female who initially presented with generalized tonic–clonic seizures, with other symptoms of Leigh syndrome becoming apparent after the seizures. A three-generation pedigree revealed no family history of mitochondrial disorders. Laboratory studies were remarkable for elevated blood lactate, alanine, and GDF15. T_2-weighted magnetic resonance imaging (MRI) revealed bilateral asymmetric signal hyperintensities in the basal ganglia, specifically in the bilateral putamen and right caudate. Magnetic resonance spectroscopy showed regionally elevated glucose and lactate. Mitochondrial respiratory chain enzyme analysis on skin fibroblasts demonstrated slightly reduced Complex I function. A 16-gene dystonia panel and chromosomal microarray analysis did not identify any disease-causing variants. Combined exome and mitochondrial genome sequencing identified the m.3685T > C (*MT-ND1* p.Tyr127His) variant with 62.3% heteroplasmy with no alternative cause for the patient's condition. Mitochondrial genome sequencing of the mother demonstrated that the m.3685T > C variant occurred de novo. The m.3685T > C variant is absent from population databases. The tyrosine 127 residue is highly conserved, and several nearby pathogenic variants in the *MT-ND1* gene have been previously associated with Leigh syndrome. We propose that the m.3685T > C variant is a novel mitochondrial DNA variant that causes Leigh syndrome, and we classify this variant as likely pathogenic based on currently available information.

[Supplemental material is available for this article.]

INTRODUCTION

Oxidative phosphorylation is the process by which ATP is formed in the mitochondria. It is characterized by an oxidative process in which electrons are transferred from NADH and $FADH_2$ to O_2 by a series of electron carriers involving Complexes I–IV (Brandt 2006). Following the oxidative process, the phosphorylation process involves the transport of protons from the inner mitochondrial matrix to the inner mitochondrial membrane space with Complex V (Brandt 2006).

Complex I is the first protein complex of the electron transport chain and is composed of 14 central protein subunits encoded by the mitochondrial as well as nuclear genomes (Vinothkumar et al. 2014). The mitochondrial genes encoding the 14 central subunits of Complex I are *MT-ND1*, *MT-ND2*, *MT-ND3*, *MT-ND4*, *MT-ND4L*, *MT-ND5*, and *MT-ND6*,

Corresponding author: rschmidt@chla.usc.edu

Ontology terms: elevated brain lactate level by MRS; focal T2 hyperintense basal ganglia lesion; generalized clonic seizures; generalized tonic seizures; hyperalaninemia

Published by Cold Spring Harbor Laboratory Press

doi:10.1101/mcs.a006136

Table 1. Confirmed pathogenic variants in the *MT-ND1* gene

Variant	Amino acid change	Disease association(s)
m.3376G > A	p.Glu24Lys	LHON MELAS overlap
m.3460G > A	p.Ala52Thr	LHON
m.3635G > A	p.Ser110Asn	LHON
m.3697G > A	p.Gly131Ser	MELAS/Leigh syndrome/LDYT/bilateral striatal necrosis
m.3700G > A	p.Ala132Thr	LHON
m.3733G > A	p.Glu143Lys	LHON
m.3890G > A	p.Arg195Gln	Progressive encephalomyopathy/Leigh syndrome/optic atrophy
m.3902_3908inv	p.Asp199_Ala201delinsGlyLysVal	Myopathy/severe lactic acidosis + cardiac abnormalities/3-MGA aciduria
m.4171C > A	p.Lys289Met	LHON/Leigh-like phenotype

(LHON) Leber hereditary optic neuropathy, (MELAS) mitochondrial encephalomyopathy, lactic acidosis, and stroke-like episodes, (LDYT) Leber's hereditary optic neuropathy and dystonia

whereas the nuclear genes encoding the 14 central subunits of Complex I are *NDUFS1*, *NDUFS2*, *NDUFS3*, *NDUFS7*, *NDUFS8*, *NDUFV1*, and *NDUFV2* (Vinothkumar et al. 2014). In addition, Complex I also has 30 accessory protein subunits, which are encoded by nuclear genes. These genes include *NDUFAB1*, *NDUFA1-3*, *NDUFA5-13*, *NDUFB1-11*, *NDUFC1-2*, *NDUFS4-6*, and *NDUFV3* (Vinothkumar et al. 2014).

Complex I is separated into three different modules: the electron input, the electron output, and the proton translocation modules (Sharma et al. 2009). The electron input module, also known as the N or dehydrogenase module, accepts electrons from NADH (Sharma et al. 2009). The electron output module, also known as the Q or hydrogenase module, delivers electrons to ubiquinone (Sharma et al. 2009). The proton translocation module, also known as the P module, pumps protons across the inner membrane (Sharma et al. 2009). The *MT-ND1*-encoded protein (NADH-ubiquinone oxidoreductase chain 1) functions within the P module and has been shown to be involved in the assembly of the entire Complex I (Sharma et al. 2009). As a whole, Complex I functions to transfer electrons from NADH to coenzyme Q10, which results in four protons being pumped out of the mitochondrial matrix into the intermembrane space (Sharma et al. 2009).

The *MT-ND1* gene has been associated with a multitude of conditions, including Leber hereditary optic neuropathy (LHON), juvenile myopathy, encephalopathy, lactic acidosis, stroke, Leber optic atrophy and dystonia, optic neuropathy, and Leigh syndrome (Lott et al. 2013). Currently, there are 13 genetic variants of *MT-ND1* that are classified as confirmed pathogenic variants in the MITOMAP database (Table 1; Lott et al. 2013) (accessed 10/8/2021).

Leigh syndrome is mainly a neurologic disorder resulting from defects in mitochondrial function (Thorburn et al. 1993). Fifty percent of the patients are deceased by 3 years old. However, for the patients who survive to adulthood, the signs and symptoms of Leigh syndrome are a continuous progression (Thorburn et al. 1993). During infancy, nonspecific signs and symptoms include diarrhea, vomiting, dysphagia, and subsequent failure to thrive (Thorburn et al. 1993). Seizures can also be seen in infants with this syndrome (Thorburn et al. 1993). Progression to muscular debilitation, including hypotonia, dystonia, and ataxia, is frequent (Thorburn et al. 1993). The muscles that control eye movements may degenerate, resulting in ophthalmoparesis and nystagmus (Thorburn et al. 1993). Hypertrophic cardiomyopathy and asymmetric septal hypertrophy may also occur (Thorburn et al. 1993). The most common cause of death in Leigh syndrome patients is respiratory failure (Thorburn et al. 1993).

RESULTS

Clinical Presentation and Family History

The patient is a 4-yr-old female with congenital left-sided diaphragmatic hernia status post-surgical repair. She has a history of generalized tonic–clonic seizures (first seizure at 16 mo of age), fine and gross motor delay and regression, speech regression, and constipation. Physical examination revealed gait abnormality, femoral anteversion, intoeing, fatigue, left hemiparesis, dystonia, and tremor. The grandparents and parents of this patient have no history of mitochondrial disorders. A formal three-generation pedigree was obtained. The parents denied consanguinity. The patient has one paternal half-sister, one full sister, and one full brother, all of whom have no significant medical histories. The father has two sisters, one of whom has a heart defect, visual problems, and speech delay. The mother has one sister and one brother, the sister having a history of mitral valve prolapse, which resolved with treatment. The maternal grandparents have hypertension.

Phenotypic Analyses

A magnetic resonance imaging (MRI) and magnetic resonance spectroscopy (MRS) of the brain were performed. The MRI revealed bilateral asymmetric basal ganglia signal hyperintensities, specifically in the right caudate and bilateral putamen (Fig. 1A). The MRS of the brain revealed high lactate and glucose levels in basal ganglia, consistent with increased mitochondrial activity and abnormal energy metabolism (Fig. 1B). The echocardiogram (ECG) and electroencephalogram (EEG) were also within normal limits. The ECG revealed normal left ventricular (LV) size and systolic function, patent foramen ovale, and normal aortic valves (AVs). The EEG, performed at 2 years of age, showed asymmetry in the posterior dominant rhythm. The posterior dominant rhythm with the patient awake and eyes closed was a moderate voltage 8–8.5 Hz activity that reacted symmetrically to eye opening but was asymmetric. The alpha rhythm appeared to be better modulated and maintained on the right. No other interhemispheric voltage or frequency asymmetries were noted. No epileptiform discharges were present. No electrographic or electroclinical seizures were recorded. Laboratory results are shown in Table 2. The urine was negative for unusual organic acids. The plasma carnitines were within normal limits. The plasma acylcarnitine profile was unremarkable. GDF15 was elevated. Blood lactate was elevated. Plasma amino acids were within normal limits with the exception of elevated alanine, which may be the result of persistently increased lactate. Mitochondrial respiratory chain enzyme analysis was performed at Baylor Genetics Laboratory using skin fibroblasts, and the results are shown in Table 3. NADH:ferricyanide dehydrogenase activity was measured to be 42% of the controlled mean. Citrate synthase activity was also found to be slightly reduced. When normalized for citrate synthase activity, the NADH:ferricyanide dehydrogenase activity is adjusted to 69%. These results suggest slightly reduced complex I function.

Genomic Analyses

A 16-gene dystonia panel performed at an outside laboratory was negative for pathogenic sequence variants and deletions/duplications. Chromosomal microarray analysis showed no clinically significant copy-number gains or losses. Exome (+mtDNA capture) sequencing was performed on peripheral blood-derived DNA with focused interpretation of genes involved in mitochondrial disorders as well as the mitochondrial genome. A mitochondrial DNA variant (m.3685T > C; Table 4) was identified with 62.3% heteroplasmy (6684 of 10,736 reads covering the position of the variant) (Fig. 2A). The m.3685T > C variant is present within the *MT-ND1* gene and is predicted to result in a p.Tyr127His missense variant. Targeted Sanger sequencing of patient's mother and two unaffected siblings (15-yr-old full sister

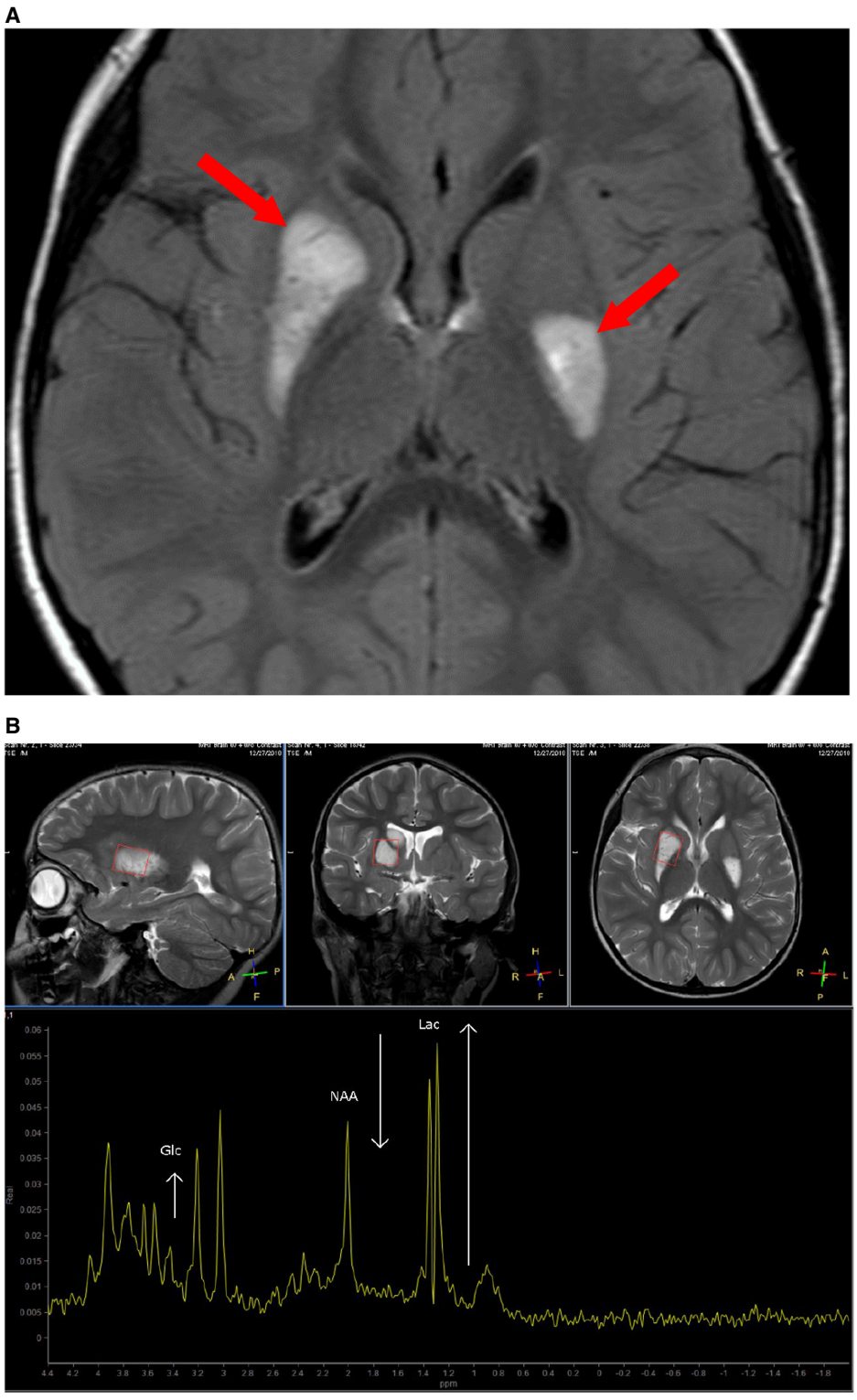

Figure 1. (*A*) Magnetic resonance imaging (MRI) shows axial T2 FLAIR with abnormal signal in the putamen bilaterally, as shown by the arrows. (*B*) Magnetic resonance spectroscopy (MRS) reveals a significantly elevated lactate (Lac), decreased N-acetylaspartate (NAA), and elevated glucose (Glc).

Table 2. Laboratory results

Test	Source	Patient values	Units	Reference range	Interpretation
Lactate	Blood	***16.9***	mg/dL	[6.0–16.0]	***Increased***
Organic acids	Urine	Negative for unusual organic acids			Normal
Acylcarnitine profile	Plasma	Very slightly increased hexadecanoyl C16			Normal
Total carnitine	Plasma	38	uMOL/L	[26–78]	Normal
Free carnitine	Plasma	29	uMOL/L	[18–61]	Normal
Carnitine esters	Plasma	9.0	uMOL/L	[7–25]	Normal
Carnitine esterified:free ratio	Plasma	0.29		[0.20–0.67]	Normal
GDF15	Plasma	***968***	pg/mL	≤750	***Increased***
Aspartic acid	Plasma	<5	uMOL/L	[1–24]	Normal
Glutamic acid	Plasma	27	uMOL/L	[5–150]	Normal
Asparagine	Plasma	37	uMOL/L	[23–112]	Normal
Serine	Plasma	134	uMOL/L	[69–187]	Normal
Glutamine	Plasma	583	uMOL/L	[254–823]	Normal
Glycine	Plasma	227	uMOL/L	[127–341]	Normal
Histidine	Plasma	72	uMOL/L	[41–125]	Normal
Threonine	Plasma	119	uMOL/L	[35–226]	Normal
Citrulline	Plasma	30	uMOL/L	[1–46]	Normal
Arginine	Plasma	51	uMOL/L	[10–140]	Normal
Alanine	Plasma	***599***	uMOL/L	[152–547]	***Increased***
Tyrosine	Plasma	41	uMOL/L	[24–115]	Normal
Methionine	Plasma	19	uMOL/L	[7–47]	Normal
Valine	Plasma	200	uMOL/L	[74–321]	Normal
Tryptophan	Plasma	39	uMOL/L	[14–79]	Normal
Phenylalanine	Plasma	41	uMOL/L	[26–91]	Normal
Isoleucine	Plasma	57	uMOL/L	[22–107]	Normal
Leucine	Plasma	98	uMOL/L	[49–216]	Normal
Ornithine	Plasma	25	uMOL/L	[10–163]	Normal
Lysine	Plasma	103	uMOL/L	[48–284]	Normal

Bold italic type designates the laboratory values that were outside of the reference range.

Table 3. Skin fibroblast respiratory chain enzyme analysis

Electron transport chain activities	ETC complexes	Value (% of mean, % of mean normalized for citrate synthase activity)	Control ± SD (nmoles/min/mg protein)
NADH:ferricyanide dehydrogenase	I	428 (42, 69)	1026 ± 196
NADH:cytochrome *c* reductase (total)	I + III	131.8 (69, 115)	190 ± 25
NADH:cytochrome *c* reductase (rotenone sensitive)	I + III	31.6 (56, 93)	56.5 ± 15
Succinate dehydrogenase	II	6.91 (99, 165)	6.98 ± 0.98
Succinate:cytochrome *c* reductase	II + III	6.33 (158, 263)	4.0 ± 0.9
Cytochrome *c* oxidase	IV	11.3 (66, 110)	17.1 ± 4.1
Citrate synthase		41 (60, 100)	67.8 ± 14.1

(ETC) Electron transport chain, (SD) standard deviation.

Table 4. Variant table

Gene	Chromosome	HGVS DNA reference	HGVS protein reference	Variant type	Predicted effect	Genotype	ClinVar ID	Parent of origin
MT-ND1	Chr MT	m.3685T > C	p.Tyr127His	Substitution	Missense	Heteroplasmic	VCV001328561.1	De novo

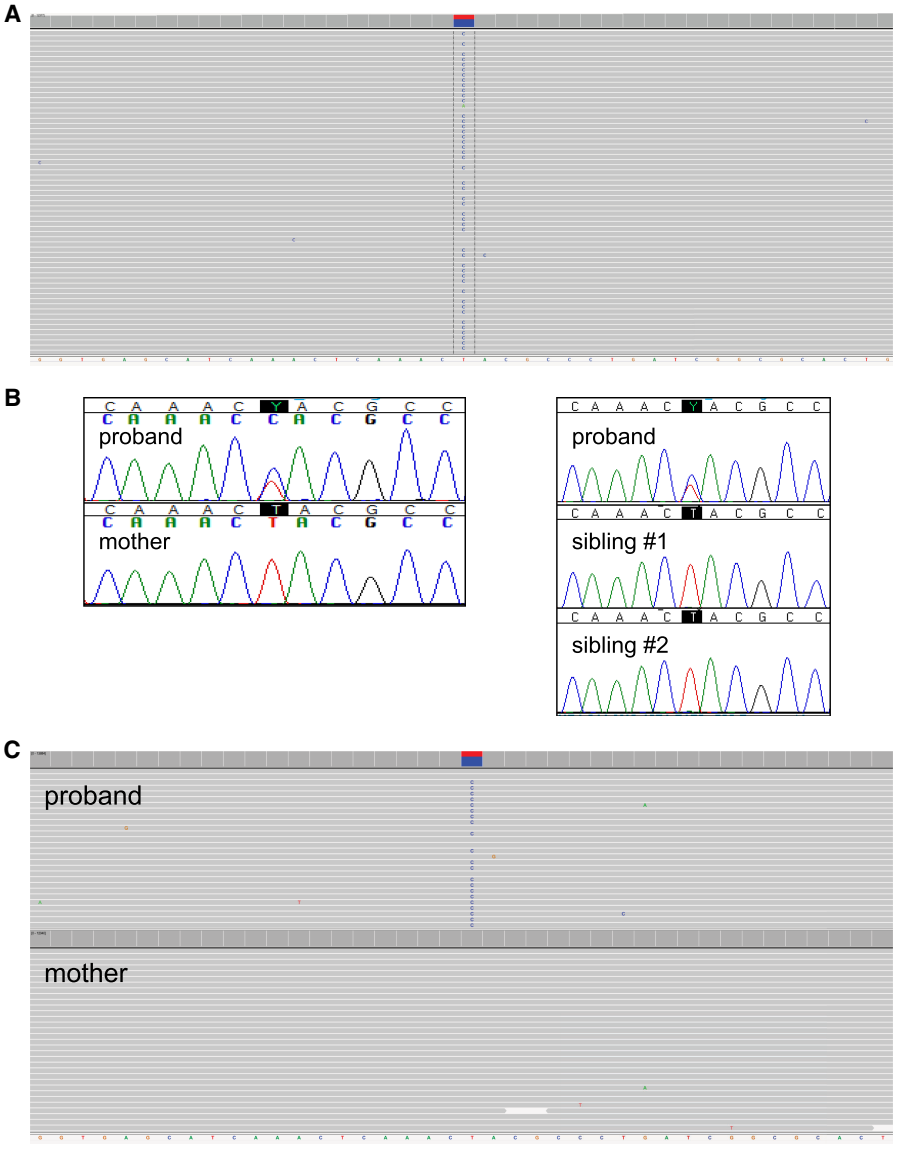

Figure 2. (*A*) Exome (+mtDNA capture) sequencing identified the m.3685T > C variant with 62% heteroplasmy. (*B*) Targeted Sanger sequencing shows that the m.3685T > C variant is not detected in the mother and two unaffected siblings. (*C*) Long-range polymerase chain reaction (PCR) followed by mitochondrial DNA (mtDNA) sequencing identified the m.3685T > C variant in 8451 of 13,388 reads (63.1% heteroplasmy) in the proband and 11 of 11,803 reads in the mother confirming that the m.3685T > C variant occurred de novo.

and 13-yr-old full brother) from peripheral blood showed no evidence for the m.3685T > C variant (Fig. 2B). Long-range polymerase chain reaction (PCR) mitochondrial DNA (mtDNA) sequencing was performed on peripheral blood as an orthogonal confirmation (Fig. 2C), which identified the m.3685T > C variant with 63.1% heteroplasmy (8451 of 13,388 reads) in the proband. In contrast, the m.3685T > C variant was not identified in the mother (11 of 11,803 reads). Whole exome analysis did not find an alternative cause for the patient's condition.

The m.3685T > C variant has not been previously reported in individuals with mitochondrial disease to our knowledge and was absent from the MITOMAP database (Lott et al. 2013) and the gnomAD v3.3.1 data set (Karczewski et al. 2020). The *MT-ND1* p.Tyr127His missense change is predicted to be pathogenic (APOGEE score = 0.6) (Castellana et al. 2017). The tyrosine 127 residue is highly evolutionarily conserved and is present in 11 other species examined down to *Drosophila melanogaster* and *Caenorhabditis elegans* using Alamut Visual analysis software (SOPHiA GENETICS). According to the specifications for mitochondrial variant interpretation (Richards et al. 2015; McCormick et al. 2020), the m.3685T > C variant is classified as likely pathogenic because it has been shown to occur de novo (PS2), is absent from control subjects (PM2), and is predicted to be damaging at the protein level (PP3).

Nearby variants (m.3697G > A [*MT-ND1* p.Gly131Ser] and m.3688G > A [*MT-ND1* p.Ala128Thr]) have been previously reported in individuals with Leigh syndrome (Valente et al. 2009; Negishi et al. 2014). The m.3697G > A variant is classified as a confirmed pathogenic variant in the MITOMAP database (Table 1; Lott et al. 2013), which has been reported in association with MELAS, Leigh Syndrome, Leber hereditary optic neuropathy and dystonia, and bilateral striatal necrosis. The m.3700G > A (p.Ala132Thr) variant is also classified as a confirmed pathogenic variant in the MITOMAP database (Table 1; Lott et al. 2013) in association with Leber hereditary optic neuropathy.

Treatment Outcomes

The patient was prescribed a mitochondrial cocktail consisting of riboflavin, levocarnitine, and coenzyme Q10 for ~2 yr. However, these medications were discontinued because of perceived lack of benefit.

DISCUSSION

The criteria used to establish the diagnosis of Leigh syndrome have undergone several revisions over time (Thorburn et al. 1993; Rahman et al. 1996; Baertling et al. 2014; Lake et al. 2016). According to Thorburn et al. (1993), a diagnosis of Leigh syndrome is suggested based on clinical features, laboratory findings, radiographic findings, histopathology, and respiratory chain enzyme studies. The clinical criteria include progressive neurologic disease, developmental delay in both motor and intellectual aspects, and signs and symptoms of brainstem and/or basal ganglia disease (nystagmus, ataxia, optic atrophy, dystonia). Laboratory findings include elevated lactate as well as elevated alanine secondary to persistently elevated lactate. Imaging findings include bilateral symmetric hypodensities in the basal ganglia on CT scan, bilateral symmetric hyperintense signal abnormality in the brain stem and/or basal ganglia by T_2-weighted MRI, and regional lactate elevation detected by MRS. Finally, biochemical testing performed on skeletal muscle and/or skin fibroblasts showing deficiency in the activity of one or more of the respiratory chain enzyme complexes is also suggestive of Leigh syndrome.

The patient described in this report initially presented with generalized tonic–clonic seizures, followed by speech and motor regression, gait abnormalities, left hemiparesis,

constipation, dystonia, and muscle hypotonia. Blood lacate, alanine, and GDF15 were found to be increased. MRI showed asymmetric hyperintensities in the basal ganglia, while MRS detected elevated lactate in this region. Enzyme studies performed on skin fibroblasts showed an apparent subtle decrease in Complex I function, but this decrease did not meet the level of reduction in enzyme activity frequently observed in respiratory chain disorders (Bernier et al. 2002). A diagnosis of suspected Leigh syndrome was given based on these findings. However, the asymmetric appearance of the MRI hyperintensities in the basal ganglia was noted to be atypical (Bonfante et al. 2016). Additionally, while skin fibroblast enzyme testing was suggestive of a subtle isolated Complex I deficiency, skeletal muscle studies are reported to be more likely to show a clear enzyme defect (Thorburn et al. 1993).

The m.3685T > C variant identified in this individual is a missense variant (p.Tyr127His) within the *MT-ND1* gene that was found to be heteroplasmic and was de novo based on testing of the mother. To the best of our knowledge, this variant is novel and has not been previously detected in individuals with disease or in population controls. Computational prediction suggests that the p.Tyr127His variant may impact protein function. While the m.3685T > C variant is currently classified as likely pathogenic by ACMG-AMP criteria with specifications for mitochondrial variants (Richards et al. 2015; McCormick et al. 2020), additional reports will be needed to definitively establish its pathogenicity. It is notable that *MT-ND1* encodes a component of Complex I, which is likely to explain the slightly reduced Complex I activity identified by enzymatic testing.

Nearby variants present in the same loop between transmembrane domains of NADH-ubiquinone oxidoreductase chain 1 [m.3688G > A (p.Ala128Thr), m.3697G > A (p.Gly131Ser), m.3700G > A (p.Ala132Thr)] were previously reported to be pathogenic for Leigh syndrome (Thorburn et al. 1993; Negishi et al. 2014). The presence of these pathogenic variants within close proximity highlights the functional importance of this loop region within the protein. The m.3697G > A (p.Gly131Ser) variant was shown to result in the disruption of the assembly of Complex I with subsequent degradation of the unincorporated subunits, which disrupted the entire process of electron transfer from NADH to ubiquinone (Kirby et al. 2004). We speculate that the m.3688G > A (p.Ala128Thr) and m.3700G > A (p.Ala132Thr) variants as well as the m.3685T > C (p.Tyr127His) variant may result in a similar disruption in the assembly of Complex I, thereby disrupting the transfer of electrons from NADH to ubiquinone.

METHODS

Neuroimaging

MRI was performed on a 3T scanner. MRS was performed with specifications as follows: single-voxel point-resolved spectroscopy (PRESS) with an echo time (TE) of 35 msec, a repetition time (TR) of 1.5 sec (for 1.5T) and 2 sec (for 3T), and 128 signal averages was used for all acquisitions.

Chromosomal Microarray

Chromosomal microarray (CMA) analysis is performed using the Affymetrix CytoScan HD microarray and analyzed using Affymetrix Chromosome Analysis Suite software using the GRCh37/hg19 genome build. This platform is sensitive to reliably detect copy-number alterations 50 kb and larger.

Sanger Sequencing

Sanger sequencing was performed using the BigDye Terminator v1.1 (Life Technologies) on an automated fluorescent sequencer (ABI 3730 Genetic Analyzer, Applied Biosystems). This assay was validated to detect variants down to 12.5% variant allele fraction. The primer sequences used were as follows (5′ → 3′): F-ATATACAACTACGCAAAGGCC, R-TAAAG GAGCCACTTATTAGTAATG. Sequences of the specific exon were compared to the NC_012920.1 mitochondrial DNA reference sequence.

Next-Generation Sequencing

The exome (+mtDNA capture) sequencing library was generated using the Agilent SureSelect Human All Exon V6 plus a custom mitochondrial genome capture kit (Falk et al. 2012). Captured DNA fragments were then sequenced using the Illumina Nextseq 500 sequencing system with 2 × 101 base pair (bp) paired-end reads. Single-nucleotide variants (SNVs) and small insertions and deletions (<10 bp) were detected by mapping and comparing the DNA sequences with the human reference genome (GRCh37/hg19). The rare nuclear DNA variants (minor allele frequency < 1%) within protein-coding regions and splice-site junctions (5 bp into introns) and any rare mitochondrial DNA variants with <0.5% MitoMap GB frequency were further annotated and analyzed using Agilent Alissa Interpret 5.2.

The long-range PCR mtDNA sequencing library was generated as described (Kaneva et al. 2020). Sequencing was performed on an Illumina MiSeq sequencer with 2 × 101 bp paired-end reads.

Sequencing coverage metrics are provided in Supplemental Table 1.

ADDITIONAL INFORMATION

Data Deposition and Access

The variant described here has been submitted to ClinVar (https://www.ncbi.nlm.nih.gov/clinvar/) and can be found under accession number VCV001328561.1.

Ethics Statement

Institutional review board approval was not required for this case report per institutional guidance as the information presented was obtained in the course of standard clinical care. The proband's mother has reviewed the manuscript and provided written consent for its publication.

Author Contributions

J.J. wrote and edited the manuscript; E.C. performed long-range PCR mtDNA sequencing and edited the manuscript; X.G. assisted with variant interpretation and edited the manuscript; B.T. provided clinical case information and edited the manuscript; M.V. provided clinical case information and edited the manuscript; W.G.M. provided clinical case information and edited the manuscript; and R.J.S. wrote and edited the manuscript and provided clinical case information and variant interpretation.

Competing Interest Statement

The authors have declared no competing interest.

Received July 30, 2021; accepted in revised form January 7, 2022.

REFERENCES

Baertling F, Rodenburg RJ, Schaper J, Smeitink JA, Koopman WJH, Mayatepek E, Morava E, Distelmaier F. 2014. A guide to diagnosis and treatment of Leigh syndrome. *J Neurol Neurosurg Psychiatry* **85:** 257–265. doi:10.1136/jnnp-2012-304426

Bernier FP, Boneh A, Dennett X, Chow CW, Cleary MA, Thorburn DR. 2002. Diagnostic criteria for respiratory chain disorders in adults and children. *Neurology* **59:** 1406–1411. doi:10.1212/01.WNL.0000033795.17156.00

Bonfante E, Koenig MK, Adejumo RB, Perinjelil V, Riascos RF. 2016. The neuroimaging of Leigh syndrome: case series and review of the literature. *Pediatr Radiol* **46:** 443–451. doi:10.1007/s00247-015-3523-5

Brandt U. 2006. Energy converting NADH:quinone oxidoreductase (complex I). *Annu Rev Biochem* **75:** 69–92. doi:10.1146/annurev.biochem.75.103004.142539

Castellana S, Fusilli C, Mazzoccoli G, Biagini T, Capocefalo D, Carella M, Vescovi AL, Mazza T. 2017. High-confidence assessment of functional impact of human mitochondrial non-synonymous genome variations by APOGEE. *PLoS Comput Biol* **13:** e1005628. doi:10.1371/journal.pcbi.1005628

Falk MJ, Pierce EA, Consugar M, Xie MH, Guadalupe M, Hardy O, Rappaport EF, Wallace DC, LeProust E, Gai X. 2012. Mitochondrial disease genetic diagnostics: optimized whole-exome analysis for all MitoCarta nuclear genes and the mitochondrial genome. *Discov Med* **14:** 389–399.

Kaneva K, Merkurjev D, Ostrow D, Ryutov A, Triska P, Stachelek K, Cobrinik D, Biegel JA, Gai X. 2020. Detection of mitochondrial DNA variants at low level heteroplasmy in pediatric CNS and extra-CNS solid tumors with three different enrichment methods. *Mitochondrion* **51:** 97–103. doi:10.1016/j.mito.2020.01.006

Karczewski KJ, Francioli LC, Tiao G, Cummings BB, Alföldi J, Wang Q, Collins RL, Laricchia KM, Ganna A, Birnbaum DP, et al. 2020. The mutational constraint spectrum quantified from variation in 141,456 humans. *Nature* **581:** 434–443. doi:10.1038/s41586-020-2308-7

Kirby DM, McFarland R, Ohtake A, Dunning C, Ryan MT, Wilson C, Ketteridge D, Turnbull DM, Thorburn DR, Taylor RW. 2004. Mutations of the mitochondrial *ND1* gene as a cause of MELAS. *J Med Genet* **41:** 784–789. doi:10.1136/jmg.2004.020537

Lake NJ, Compton AG, Rahman S, Thorburn DR. 2016. Leigh syndrome: one disorder, more than 75 monogenic causes. *Ann Neurol* **79:** 190–203. doi:10.1002/ana.24551

Lott MT, Leipzig JN, Derbeneva O, Xie HM, Chalkia D, Sarmady M, Procaccio V, Wallace DC. 2013. mtDNA variation and analysis using Mitomap and Mitomaster. *Curr Protoc Bioinformatics* **44:** 1.23.21–1.23.26. doi:10.1002/0471250953.bi0123s44

McCormick EM, Lott MT, Dulik MC, Shen L, Attimonelli M, Vitale O, Karaa A, Bai R, Pineda-Alvarez DE, Singh LN, et al. 2020. Specifications of the ACMG/AMP standards and guidelines for mitochondrial DNA variant interpretation. *Hum Mutat* **41:** 2028–2057. doi:10.1002/humu.24107

Negishi Y, Hattori A, Takeshita E, Sakai C, Ando N, Ito T, Goto Y-I, Saitoh S. 2014. Homoplasmy of a mitochondrial 3697G>A mutation causes Leigh syndrome. *J Hum Genet* **59:** 405–407. doi:10.1038/jhg.2014.41

Rahman S, Blok RB, Dahl HH, Danks DM, Kirby DM, Chow CW, Christodoulou J, Thorburn DR. 1996. Leigh syndrome: clinical features and biochemical and DNA abnormalities. *Ann Neurol* **39:** 343–351. doi:10.1002/ana.410390311

Richards S, Aziz N, Bale S, Bick D, Das S, Gastier-Foster J, Grody WW, Hegde M, Lyon E, Spector E, et al. 2015. Standards and guidelines for the interpretation of sequence variants: a joint consensus recommendation of the American College of Medical Genetics and Genomics and the Association for Molecular Pathology. *Genet Med* **17:** 405–424. doi:10.1038/gim.2015.30

Sharma LK, Lu J, Bai Y. 2009. Mitochondrial respiratory complex I: structure, function and implication in human diseases. *Curr Med Chem* **16:** 1266–1277. doi:10.2174/092986709787846578

Thorburn DR, Rahman J, Rahman S. 1993. Mitochondrial DNA-associated Leigh syndrome and NARP. In *GeneReviews®* (ed. Adam MP, Ardinger HH, Pagon RA, et al.). University of Washington, Seattle.

Valente L, Piga D, Lamantea E, Carrara F, Uziel G, Cudia P, Zani A, Farina L, Morandi L, Mora M, et al. 2009. Identification of novel mutations in five patients with mitochondrial encephalomyopathy. *Biochim Biophys Acta* **1787:** 491–501. doi:10.1016/j.bbabio.2008.10.001

Vinothkumar KR, Zhu J, Hirst J. 2014. Architecture of mammalian respiratory complex I. *Nature* **515:** 80–84. doi:10.1038/nature13686